Materials Research Bulletin 60 (2014) 446–452

Contents lists available at ScienceDirect

Materials Research Bulletin

journal homepage: www.elsevier.com/locate/matresbu

Activation behavior and dielectric relaxation of nanocrystalline zinc ferrite

S. Choudhury [a], M. Sinha [b], H. Dutta [c], M.K. Mandal [a], S.K. Pradhan [b], A.K. Meikap [a,*]

[a] Department of Physics, National Institute of Technology, Durgapur, Burdwan 713209, West Bengal, India
[b] Department of Physics, The University of Burdwan, Golapbag, Burdwan 713104, West Bengal, India
[c] Department of Physics, Vivekananda College, Burdwan 713103, West Bengal, India

ARTICLE INFO

Article history:
Received 8 October 2013
Received in revised form 24 March 2014
Accepted 1 September 2014
Available online 3 September 2014

Keywords:
A. Zinc Ferrite
A. Nanostructures
C. X-ray diffraction
D. Dielectric properties
D. Microstructure

ABSTRACT

We report the ac conductivity and dielectric relaxation studies of nanocrystalline zinc ferrite prepared by the ball milling. The real part of the complex ac conductivity is found to follow the universal dielectric response $\sigma'(f) \propto T^n f^s$ and values of both s and n show an anomalous behavior. Both the magnitude of the temperature exponent 'n' and thermal activation energy for ac conduction strongly depends on frequencies. The dielectric constant exhibits strong temperature dependence at higher temperature and lower frequencies. The dielectric properties of the samples have been analyzed in terms of electric modulus vector. The complex impedance has also been modeled by an ideal equivalent circuit consisting of grain and grain boundary resistances and capacitances. Considering the formation of Schottky diode at the metallic electrode and semiconductor junction, the diode parameters like built in voltage and space charge density have been extracted from the capacitance-voltage characteristics.

1. Introduction

The magnetic nanoparticles have been intensively investigated in the past few years because of their technological applications in magnetic recording, information storing, data processing devices, magnetic resonance imaging and drug delivery systems [1–5] and their relevance in fundamental physics. The physical properties of nanostructure ferrites are quite different from their bulk counterparts. It is well known that magnetic properties of nanosized ferrites are strongly influenced by the particle size, morphology, structure and cation distributions. These parameters are very sensitive to the preparation techniques.

In general, ferrites are metal oxides in which magnetic ions are arranged in such a manner, which produces a net magnetization. The term spinel is widely used to identify the compounds with general formula MFe_2O_4 (M is the divalent metal ion). The structural formula of zinc ferrite is usually written as $(Zn_{1-\delta}^{2+}Fe_{\delta}^{3+})[Zn_{\delta}^{2+}Fe_{2-\delta}^{3+}]O_4^{2-}$, where round () and square [] brackets denote T (tetrahedral) and O (octahedral) sites of the coordination respectively and δ represents the degree of inversion i.e., the fraction of T sites occupied by Fe cations. Different magnetic ordering exists in these materials due to various kinds of super-exchange interactions between T and O site cations. This magnetic ordering is also influenced greatly by reducing the particle size to nanometer range [6,7]. Spinel ferrite has attracted considerable attention in the last few years due to their potential applications in nanoscience and technology [8–12]. Nanocrystalline ferrite materials have made them an object of interest for many researchers due to their unusual properties originating from the presence of large number of atoms at the grain boundaries or interfacial boundaries.

An extensive investigation has been made to explore the properties of a large number of ferrites describing the preparation and characterization of structural and magnetic properties like magnetization measurement, Mossbauer spectroscopy and neutron scattering [13–26]. Electrical and dielectric properties of zinc ferrite above room temperature are reported in some cases [26–28]. However, systematic studies on dielectric response and complex electric modulus of the nanocrystalline zinc ferrite is still lacking. The investigation of the electrical properties of ferrites can reveal useful information regarding the behavior of localized carriers, which provide better understanding of the mechanism of dielectric polarization. A strong correlation has been observed between the dielectric properties and the conduction mechanism of these materials [29]. The aim of this work is to investigate ac conductivity, complex electric modulus and complex impedance of

* Corresponding author. Tel.: +91 343 2546808; fax: +91 343 2547375.
E-mail address: meikapnitd@yahoo.com (A.K. Meikap).

http://dx.doi.org/10.1016/j.materresbull.2014.09.002
0025-5408/

the nanocrystalline zinc ferrite for valuable information on its electrical properties which help to elaborate the range of practical applications of zinc ferrite in different important fields.

The present work reports the preparation, characterization and electrical transport properties of nanocrystalline zinc ferrite. An extensive dielectric response of zinc ferrite has been made in the temperature range 298–523 K and in the frequency range from 20 Hz to 1 MHz.

2. Sample preparation and experimental technique

Accurately weighed (1:1 molar ratio) $Fe(NO_3)_3$ and $Zn(NO_3)_2$ (purity >99%) powders was mixed in distilled water and kept for several hours on magnetic stirrer for a homogeneous mixture, without any residue left over. The homogeneous mixture was then subjected to heat at 300 °C for another couple of hours to obtain a solid powder mixture. This powder was then kept in the furnace at 800 °C for 1 h for the formation $ZnFe_2O_4$ phase. Obtained powder, termed as unmilled sample, was ball milled for different durations for obtaining nanocrystalline Zn-ferrite samples of different particle sizes. Powder milled in air in a planetary ball mill (Fritsch, GmbH) using 80 ml chrome steel vial and 30 balls made of same material. The BPMR (ball to powder mass ratio) was kept at 40:1 and rpm of the rotating disk was 300 to obtain a better impact between powder grains and milling media.

The X-ray powder diffraction profiles of the unmilled mixture and ball milled samples were recorded using Ni-filtered CuKα radiation from a highly stabilized and automated Philips X-ray generator (PW 1830) operated at 40 kV and 20 mA. The generator is coupled with a Philips X-ray powder diffractometer consisting of a PW 3710 mpd controller, PW 1050/51 goniometer, and a proportional counter. For this experiment, 1° divergence slit, 0.2 mm receiving slit, 1° scatter slit and 5° soller slit system were used. The step-scan data (of step size 0.05° 2θ and counting time 5–10 s depending on the peak intensity) were recorded for the entire angular range 15–80° 2θ. To measure ac response, samples were prepared as 1 cm diameter pellets by pressing the powder at 500 MPa under a hydraulic press. The detailed experimental technique is described by Ghosh et al. [30].

3. Result and discussion

Fig. 1 shows the X-ray powder diffraction patterns of unmilled and ball milled samples. The major phase in unmilled powder is identified as $ZnFe_2O_4$ (ICSD Ref. code #01-073-1963; cubic, space group: Fd-3 m, $a = 8.3500$ Å) and the minor phase is as ZnO (ICSD Ref. code #01-089-0510; hexagonal, space group: $P6_3mc$, $a = 3.2488$ Å, $c = 5.2054$ Å). Both these phases are well crystalline and some peaks are overlapped. In the course of ball milling the powder patterns are modified towards the major Zn-ferrite phase and the peak broadening increases with increasing milling time.

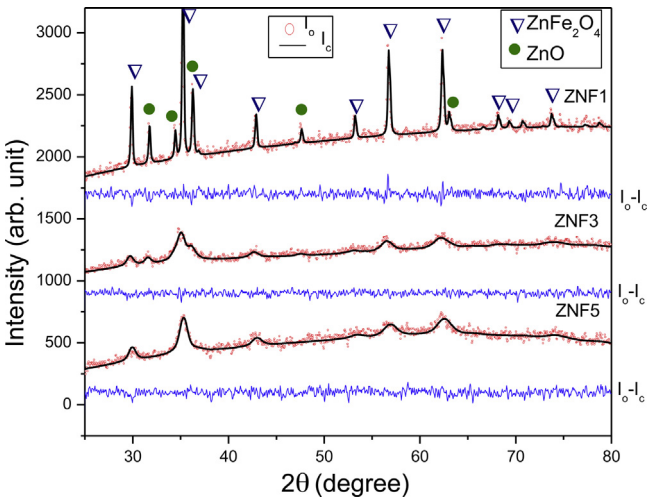

Fig. 1. Rietveld output of X-ray powder diffraction patterns of unmilled and ball milled zinc ferrite powders prepared by chemical route. Experimental data points are shown as hollow circles, while refined simulated patterns are shown as continuous lines. The difference between the experimental data (I_O) and the fitted simulated pattern (I_C) is shown as a continuous line (I_O–I_C) under each diffraction pattern.

It seems that the minor ZnO phase is incorporated into ferrite matrix slowly with increasing milling time and the initial mixture becomes more homogeneous with increasing milling time. To estimate the accurate structure and microstructure parameters of unmilled and ball milled samples, the Rietveld structure refinement [31–33] method has been adopted in the present case. The residue of fittings (I_O–I_C) between observed intensities (I_O) and calculated patterns (I_C) are shown at the bottom of the respective patterns. All XRD patterns are fitted considering the contribution of the major Zn ferrite and minor ZnO phases. The results tabulated in Table 1 reveals that the mol fraction of major ferrite phase increases with increasing milling time and after 2 h of milling, the ferrite phase turned into an almost stoichiometric (~99%) one. The detailed discussion of the XRD analysis is given in our previous work [28].

The electrical conductivity in ferrite samples can be explained by the electron exchange between ions of the same elements, which are present in more than one valance state and distributed randomly over the crystal. In this system, the conductivity depends on the number of the Fe^{2+} ions in the octahedral sites. The frequency dependent conductivity of the investigated samples are measured in the frequency range from 20 Hz to 1 MHz and in the temperature range $298 \leq T \leq 523$ K. It is observed from the measured data that at low frequencies the dc contribution plays a dominant role and conductivity becomes frequency independent, but at higher frequency conductivity becomes frequency

Table 1
Microstructure parameters of unmilled and ball milled Zinc ferrite (prepared by chemical route) revealed by Rietveld's X-ray powder structure refinement analysis.

Milling time	Phase present	Mole particle ±(10^{-3}–10^{-2})[a]	Lattice parameter ±(10^{-5}–10^{-3})[a]			Particle size (nm) ±(10^{-2}–10^{-1})[a]
			a (nm)	*b* (nm)	*c* (nm)	
ZNF1	Zn-ferrite	0.780	0.8431	0.8431	0.8431	108.5
0 min	ZnO	0.220	0.3246	0.3246	0.5201	150.3
ZNF3	Zn-ferrite	0.884	0.8462	0.8462	0.8462	8.7
30 min	ZnO	0.116	0.3242	0.3242	0.5188	99.8
ZNF3	Zn-ferrite	0.989	0.8416	0.8416	0.8416	9.8
2 h	ZnO	0.11	0.3182	0.3182	0.5119	145.4

[a] Error limits.